after which time 5-μL aliquots were taken to measure the PLA_2 activity (final concentration of drug under assay conditions: 0.25 μM). Controls and samples which had been preincubated with luffariellolide, both treated with or without $NaBH_4$, were dialyzed against HEPES buffer (pH 7.4, 0 °C, 17 h with two buffer changes), and the postdialysis activity was measured. The samples were then diluted 2-fold with HEPES or with hydroxylamine in HEPES (final concentration of hydroxylamine: 50 mM) and incubated at 41 °C for 2 h, after which time 10-μL aliquots were taken to measure the PLA_2 activity.

Acknowledgment. This research was sponsored in part by NOAA, National Sea Grant College Program, Department of Commerce, under Grant NA89AA-D-SG138, Projects R/MP-46 (D.J.F.) and R/MP-47 (R.J.), through the California Sea Grant College, and in part by the California State Resources Agency.

Structure and Reactivity of Lithium Diisopropylamide in the Presence of *N,N,N',N'*-Tetramethylethylenediamine

Max P. Bernstein,[†] Floyd E. Romesberg,[†] David J. Fuller,[†] Aidan T. Harrison,[†] David B. Collum,*[,†] Qi-Yong Liu,[‡] and Paul G. Williard*[,‡]

Contribution from the Department of Chemistry, Baker Laboratory, Cornell University, Ithaca, New York 14853-1301, and the Department of Chemistry, Brown University, Providence, Rhode Island 02912. *Received August 12, 1991*

Abstract: Lithium diisopropylamide (LDA) crystallizes from *N,N,N',N'*-tetramethylethylenediamine (TMEDA)/hexane mixtures as an infinite array of dimers linked by bridging (nonchelating) TMEDA ligands. ^6Li and ^{15}N NMR spectroscopic studies reveal that LDA in neat TMEDA exists as a cyclic dimer bearing a single η^1-coordinated TMEDA ligand on each lithium. The equilibrium of solvent-free LDA and the TMEDA-solvated dimer shows a very strong temperature dependence. TMEDA coordinates readily only at low temperature. High TMEDA concentrations are required to saturate the lithium coordination spheres at ambient temperatures. One equivalent of THF readily displaces TMEDA from the coordination sphere to produce the dimeric LDA/THF solvate characterized previously. Kinetics of metalation of 2-methylcyclohexanone *N,N*-dimethylhydrazone monitored by Fourier-transform infrared (FT-IR) spectroscopy are consistent with a rapid, spectroscopically undetectable dimer-monomer preequilibrium followed by rate-limiting proton transfer. The reaction rate is independent of the TMEDA concentration. Related spectroscopic and rate studies using dimethylethylamine lacking the capacity to chelate show strong parallels with the TMEDA data. We conclude that TMEDA chelates of LDA are of no measurable consequence throughout the reaction coordinate. MNDO calculations of THF and TMEDA solvates of Me_2NLi and LDA monomers and dimers qualitatively support the conclusions derived from the experimental data.

Introduction

Upon taking a casual survey of the literature of organolithium chemistry, one is struck by the central role played by *N,N,N',N'*-tetramethylethylenediamine (TMEDA; **1**). The crystallographic literature is replete with the Li-TMEDA chelate substructure **2**.[1] The kinetic consequences of TMEDA chelates are even more prominent. TMEDA dramatically accelerates organolithium reaction rates, improves product yields, and alters product distributions.[2] The consensus is that the two Lewis basic dimethylamino moieties function cooperatively to make TMEDA a truly outstanding ligand for the Li^+ ion.

We describe below structure and reactivity studies of lithium diisopropylamide (LDA) in the presence of TMEDA. An X-ray crystal structure reveals that LDA crystallizes from TMEDA/hexane as an infinite array of dimer units connected by η^1-linkages (e.g., **3**). We further demonstrate that TMEDA-solvated LDA is dimeric and desolvates at ambient temperatures *even in the absence of other donor ligands.* Less direct evidence implicates dimer **4** rather than the anticipated doubly chelated dimer **5** as the stable solution structure in the limit of high TMEDA concentration. Rate studies of the metalation of *N,N*-dimethylhydrazone **6** by LDA in neat TMEDA are interpreted in the context of the mechanism illustrated in Scheme I without invoking TMEDA chelates at any point along the reaction coordinate.[3]

Results

We will begin the Results section with a discussion of NMR spectroscopic studies of LDA in the presence of TMEDA. It is instructive to note, however, that the metalation rate data described subsequently signaled several structural subtleties that may have otherwise gone undetected.

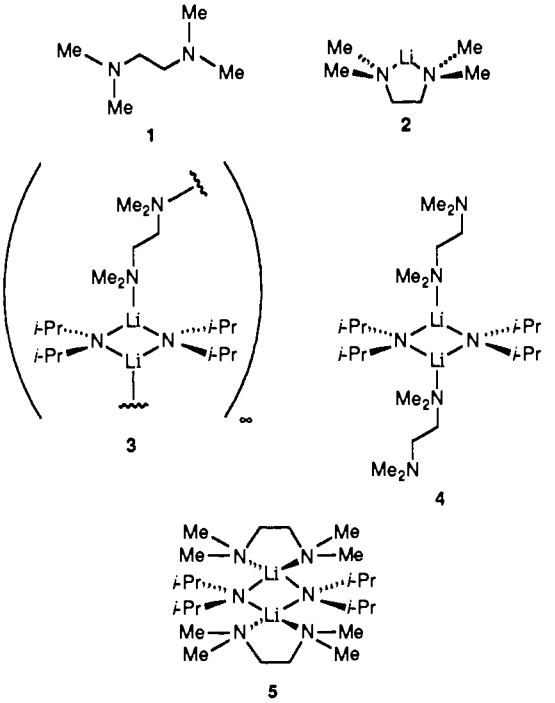

Solution Structure of LDA in TMEDA. ^6Li and ^{15}N NMR spectra of analytically pure [^6Li,^{15}N]LDA[4] dissolved in neat

[†] Cornell University.
[‡] Brown University.

(1) Schleyer, P. v. R. *Pure Appl. Chem.* **1984**, *56*, 151. Williard, P. G. In *Comprehensive Organic Synthesis*; Pergamon: New York, in press. Boche, G. *Angew. Chem., Int. Ed. Engl.* **1989**, *28*, 277.

0002-7863/92/1514-5100$03.00/0

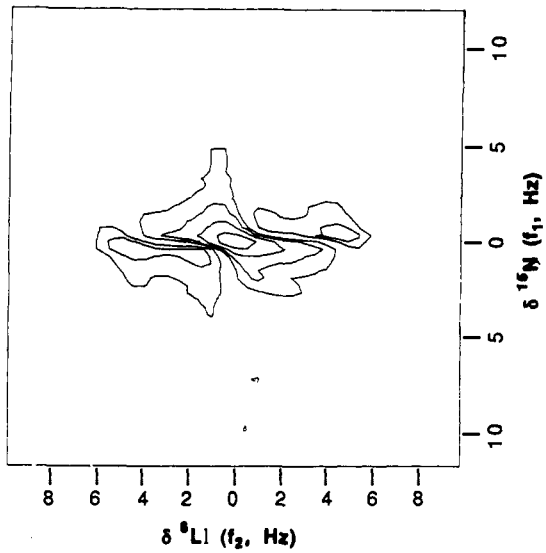

Figure 1. ^{6}Li-detected ^{15}N zero-quantum NMR spectrum of a 0.20 M solution of [^{6}Li,^{15}N]LDA in pentane containing 10 equiv of TMEDA (per Li). The spectrum was recorded at −48 °C on a Bruker AC 300 spectrometer operating at 44.17 and 30.42 MHz for ^{6}Li and ^{15}N (respectively) with hardware modifications as described previously.[2] Data were processed in phase-sensitive mode. Digital resolution in f_1 prior to zero filling is 0.75 Hz.

Scheme I

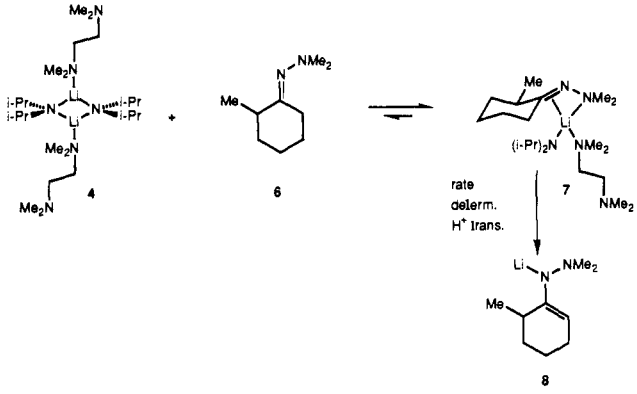

TMEDA at −55 °C display a 1:2:1 triplet (δ 2.03 ppm, J_{Li-N} = 4.5 Hz) and 1:2:3:2:1 quintet (δ 73.4 ppm, J_{Li-N} = 4.9 Hz), respectively, indicating that the cyclic oligomer structure remains intact. Previous suggestions that the highly symmetric lithium dialkylamide cyclic oligomers are dimers were based solely on mounting indirect evidence.[5] However, inverse-detected ^{15}N homonuclear zero-quantum NMR spectroscopy allows for the distinction of dimers from higher oligomers to be made directly.[6]

Employing the pulse sequence of Müller[7] and Bodenhausen and Ruben,[8] homonuclear ^{15}N two-spin coherence (a mixture of zero- and double-quantum coherence) is prepared from the two ^{15}N spins

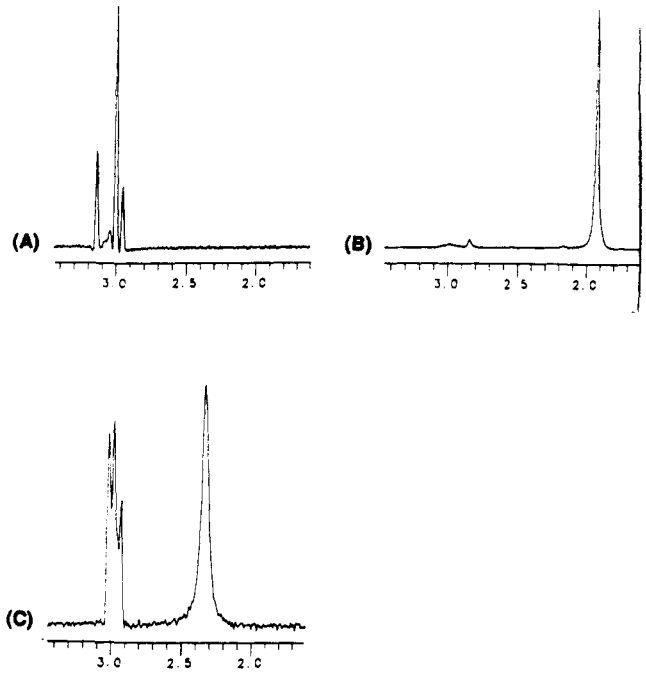

Figure 2. ^{6}Li NMR spectra of 0.13 M [^{6}Li]LDA in hexane: (A) −65 °C; (B) −100 °C, 1.0 equiv of TMEDA; (C) −40 °C, 1.0 equiv of TMEDA.

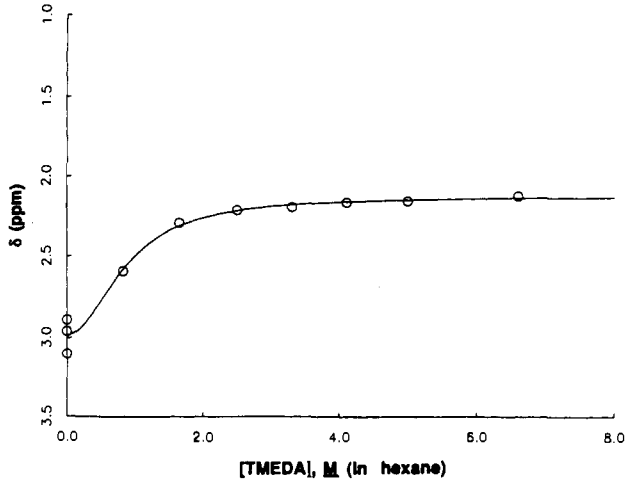

Figure 3. Time-averaged ^{6}Li chemical shifts measured at 20 °C on 0.13 M solutions of [^{6}Li]LDA in hexane containing varying concentrations of added TMEDA.

neighboring a ^{6}Li atom in a ^{6}Li–^{15}N doubly-labeled lithium dialkylamide cyclic oligomer. During the evolution period of the experiment, the zero-quantum coherence will evolve under scalar coupling only to ^{6}Li spins that are coupled to one, but not to both, ^{15}N spins. For a lithium amide dimer, all ^{6}Li spins coupled to ^{15}N spins involved in the two-spin coherence are coupled to *both* ^{15}N spins. As a consequence, the coupling pattern will be a singlet along the f_1 dimension of the two-dimensional spectrum. In the case of higher cyclic oligomers, there exist two ^{6}Li spins that are coupled to one, but not both, ^{15}N spins. The zero-quantum coherence will develop scalar coupling to the two nonshared ^{6}Li spins, resulting in a 1:2:3:2:1 pattern along the f_1 dimension. As a result of a refocusing delay employed prior to detection, all oligomers will be a 1:−2:1 pattern along the f_2 dimension. The results of the experiment as applied to [^{6}Li,^{15}N]LDA in TMEDA/pentane are illustrated in Figure 1. The absence of coupling in the f_1 (^{15}N) dimension is consistent with a dimer and inconsistent with trimers or higher oligomers.

Spectroscopic studies of LDA at low TMEDA concentrations reveal details of the TMEDA–LDA interaction that were unexpected (Figure 2). Solvent-free LDA in hexane exists as a mixture

(2) (a) *Polyamine-Chelated Alkali Metal Compounds*; Langer, A. W., Jr., Ed.; American Chemical Society: Washington, 1974. *Polyamine-Chelated Alkali Metal Compounds*; Langer, A. W., Jr., Ed.; American Chemical Society: Washington, 1974. (b) Szwarc, M. *Carbanions, Living Polymers, and Electron Transfer Processes*; Interscience: New York, 1968. (c) Snieckus, V. *Chem. Rev.* **1990**, *90*, 879. (d) Gschwend, H. W.; Rodriguez, H. R. *Org. React.* **1979**, *26*, 1. (e) Seebach, D. *Angew. Chem., Int. Ed. Engl.* **1988**, *27*, 1624. (f) Beak, P. *Chem. Rev.* **1984**, *84*, 471. (g) Beak, P.; Meyers, A. I. *Acc. Chem. Res.* **1986**, *19*, 356.

(3) Galiano-Roth, A. S.; Collum, D. B. *J. Am. Chem. Soc.* **1989**, *111*, 6772.

(4) Kim, Y.-J.; Bernstein, M. P.; Galiano-Roth, A. S.; Romesberg, F. E.; Williard, P. G.; Fuller, D. J.; Harrison, A. T.; Collum, D. B. *J. Org. Chem.* **1991**, *56*, 4435.

(5) Hall, P.; Gilchrist, J. H.; Harrison, A. T.; Fuller, D. J.; Collum, D. B. *J. Am. Chem. Soc.* **1991**, *113*, 9575. Romesberg, F. E.; Collum, D. B. *J. Am. Chem. Soc.* **1992**, *114*, 2112.

(6) Gilchrist, J. H.; Collum, D. B. *J. Am. Chem. Soc.* **1992**, *114*, 794.

(7) Müller, L. *J. Am. Chem. Soc.* **1979**, *101*, 4481.

(8) Bodenhausen, G.; Ruben, D. J. *Chem. Phys. Lett.* **1980**, *69*, 185.

Table I. Carbon-13 NMR Spectroscopic Data of 0.13 M LDA in Toluene-d_8 at −90 and 20 °C

substrates (1.0 equiv of additive)	temp, °C	resonances[a] LDA CH	LDA CH_3	TMEDA CH_2	TMEDA CH_3	THF C_α	THF C_β
LDA	−90	48.7	26.9				
		47.7	26.6				
		47.5	25.4				
LDA/TMEDA	−90	49.4	27.9	57.5[b]	46.1		
LDA/THF	−90	52.1	27.3			67.8	25.4
LDA/TMEDA/THF	−90	52.2	27.4	58.1	46.1	68.2	25.1
TMEDA	−90			58.1	46.0		
THF	−90					68.0	25.8
LDA	20	50.7	28.1				
		49.3	27.5				
		48.4	27.1				
		48.3	27.0				
LDA/TMEDA	20	50.4[c]	27.8[c]	58.2	45.9		
			27.0				
LDA/THF	20	52.0	27.9			68.2	25.6
LDA/TMEDA/THF	20	52.0	27.9	58.3	46.0	68.2	25.5
TMEDA	20			58.5	45.9		
THF	20					68.2	25.5

[a] Resonances of traces of free $(i\text{-Pr})_2NH$ are relatively constant in all samples. [b] Very broad ($\nu_{1/2}$ = 39 Hz) compared to CH_2 of free TMEDA ($\nu_{1/2}$ = 7 Hz). [c] Very broad.

of three to five cyclic oligomers exhibiting a characteristic cluster of five resonances (three major and two very minor) in the downfield region of the ^{6}Li NMR spectrum (δ 2.7–3.3 ppm; Figure 2A) as described previously.[4] The ^{6}Li spectrum of an LDA/hexane solution containing 1.0 equiv of TMEDA at −100 °C reveals predominantly the TMEDA solvate (δ 1.96 ppm; Figure 2B). However, the metalation rate studies described below were effected 120 °C higher than the spectroscopic measurements. At elevated temperatures, a large negative entropy of solvation in conjunction with a decreasing enthalpic contribution should substantially disfavor metal ion solvation. Indeed, incremental temperature increases to 20 °C show very clear evidence of a temperature-dependent desolvation (cf. Figure 2C). A plot of the time-averaged ^{6}Li chemical shift of [^{6}Li]LDA at 20 °C as a function of TMEDA concentration (in hexane) shows an asymptotic approach to the chemical shift of the LDA/TMEDA solvate only at substantially elevated TMEDA concentrations (Figure 3).[9] The double-labeling studies described above demonstrate that *the solvent-dependent equilibrium involves solvation of the LDA dimer rather than deaggregation to monomer.* From the equilibrium expression in eq 1 (S = solvent, $AS_n = (LDA)_2{\cdot}S_n$, A = solvent-free LDA) and the expression relating time-averaged chemical shifts to relative concentrations (eq 2), one obtains the expression in eq 3. The nonlinear least-squares fit in Figure 3 provides $K_{eq} = 1.3 \pm 0.3$.[10]

$$[AS_n]/[A] = K_{eq}[S]^n \quad (1)$$

$$[AS_n]/[A] = (\delta_{obs} - \delta_A)/(\delta_{AS_n} - \delta_{obs}) \quad (2)$$

$$\delta_{obs} = (K_{eq}\delta_{AS_n}[S]^n + \delta_A)/(1 - K_{eq}[S]^n) \quad (3)$$

(9) The desolvation at elevated temperatures occurred with concomitant growth of the majority of unsolvated oligomers of LDA. However, one resonance assumed the chemical shift characteristic of an unsolvated oligomer through a TMEDA-concentration-dependent shifting (migration). Although this was not studied in detail, it may be a consequence of rapid solvent exchange between the unsolvated, monosolvated, and disolvated dimer in conjunction with a slow exchange of the dimer with the higher oligomers.

(10) Nonlinear least-squares fit of the spectroscopic data to eq 3 were poorly behaved when the order in THF (n) was left as an adjustable parameter; the system was insufficiently defined to allow for such a determination of the shape of the fall-off region about the inflection point. Furthermore, the distribution of oligomers of solvent-free LDA precludes a rigorous treatment. Accordingly, we restricted the model to one molecule of TMEDA coordinated per lithium (enforcing n = 2) and report the values of K_{eq} without units. An operationally equivalent restriction placed on the kinetic fits allows for a reasonable comparison of the value of K_{eq} from the spectroscopic and kinetic data.

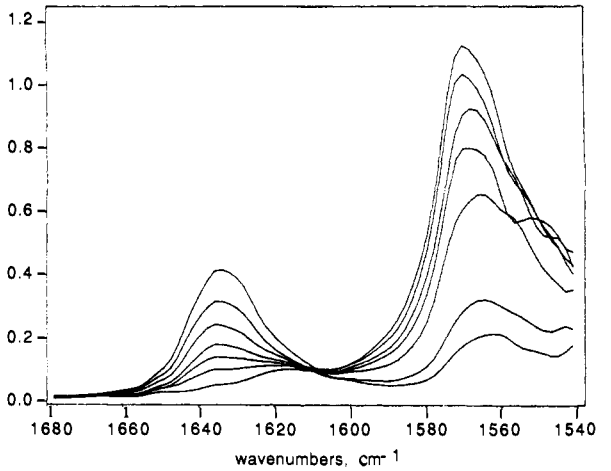

Figure 4. FT-IR spectroscopic analysis of the lithiation of hydrazone **6** (0.1 M) by LDA (0.13 M) in neat TMEDA at 20.0 ± 0.1 °C. The curves correspond to time increments in the range 60–2000 s.

Solvation of LDA by TMEDA at ambient temperatures is surprisingly unfavorable given the absence of other donor ligands to compete for the free coordination sites. As a comparison, we note that quantitative solvation of LDA by 2.0 equiv of THF is observed even at elevated temperatures.[11] *Thus, THF has a substantially greater affinity toward LDA than does TMEDA.* Additional support of this conclusion is described below.

The suggestion that LDA is solvated by TMEDA only in the absence of THF and only at reduced temperatures is supported by ^{13}C NMR spectroscopy (Table I). Previous studies of organolithium solvation by TMEDA using ^{13}C NMR spectroscopy revealed substantial chemical shift perturbations of both the methyl and methylene resonances of the TMEDA ligand upon coordination to lithium.[2a] Slow exchange of free and coordinated TMEDA has been observed.[12] The ^{13}C NMR spectrum of LDA/hexane in the absence of TMEDA displays several discrete sets of resonances corresponding to the unsolvated oligomers (Table I). In the presence of 1.0 equiv of TMEDA (toluene-d_8, −90 °C), a single set of LDA resonances is consistent with the formation of the TMEDA solvate observed by ^{6}Li and ^{15}N NMR spectroscopy. The TMEDA methylene carbon resonance displays a minor but measurable (0.6 ppm) change in chemical shift and substantial broadening ($\nu_{1/2}$ = 39 Hz). The TMEDA methyl resonance is not measurably influenced by coordination. In the presence of 2.0 equiv of TMEDA per Li, a single pair of TMEDA resonances indicates that ligand exchange is rapid down to −90 °C. Upon incremental warming of the sample to ambient temperature, a desolvation is evidenced by the appearance of the multiple sets of ^{13}C resonances characteristic of unsolvated LDA. In addition, the chemical shifts of the TMEDA resonances become indistinguishable from those of free TMEDA. To confirm the higher affinity of THF than TMEDA for LDA, we recorded the ^{13}C NMR spectrum of a 1:1:1 mixture of LDA/THF/TMEDA in toluene-d_8 at both −90 and 20 °C. The ^{13}C chemical shifts and peak widths of the TMEDA carbon resonances are fully consistent with only uncoordinated TMEDA in solution; *THF readily displaces TMEDA from the LDA dimer.*[13]

Hydrazone Metalation. Infrared Spectroscopy. Previous studies of the lithiation of *N,N*-dimethylhydrazone **6** by LDA in THF provide foundations for studying the influence of TMEDA on the structure and reactivity of LDA.[3] One observes no measurable effect of added LDA on the intensity or position of the infrared

(11) The quantitative solvation of LDA by low concentrations of THF at ambient temperatures had previously been inferred from solubility and kinetic data (ref 3).

(12) Fraenkel, G.; Chow, A.; Winchester, W. R. *J. Am. Chem. Soc.* **1990**, *112*, 1382.

(13) For comprehensive reviews of the structures of N-lithiated species, see: Gregory, K.; Schleyer, P. v. R.; Snaith, R. *Adv. Organomet. Chem.*, in press. Mulvey, R. E. *Chem. Soc. Rev.* **1991**, *20*, 167.

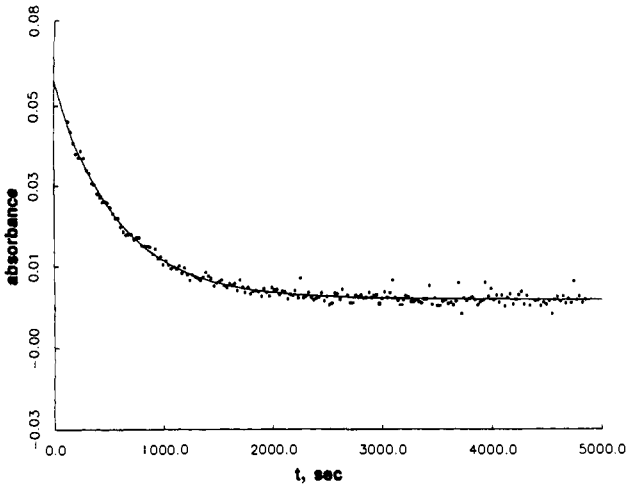

Figure 5. Representative raw data set for the lithiation of hydrazone **6** (0.004 M) by LDA (0.13 M) in 1:1 TMEDA/THF. The nonlinear least-squares fit derives from the general first-order expression $abs - abs_o = (abs_\infty - abs_o)(1 - e^{-kt})$.

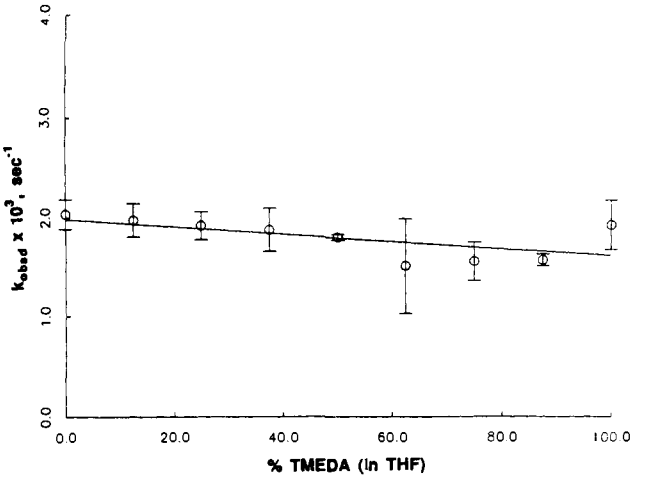

Figure 6. Plot of k_{obsd} versus [TMEDA] in THF cosolvent for the metalation of hydrazone **6** (0.004 M) by LDA (0.13 M) at 20.0 ± 0.1 °C. The solid line depicts the result of a linear least-squares fit weighted to $1/\sigma^2$.

absorbance of **6** (1636 cm^{-1}) in hexane, TMEDA/hexane, THF, or TMEDA/THF.[14] Furthermore, ^{6}Li NMR spectroscopic analysis of a solution 0.10 M solvent-free [^{6}Li]LDA and 0.20 M **6** in hexane at −95 °C reveals solvent-free oligomers as well as a limited concentration (δ 2.19 ppm, approximately 20–25%) of a species attributable to an LDA–hydrazone complex. Therefore, under the conditions of the kinetic analysis described below (20 °C, 0.004 M **6**, 0–6.6 M TMEDA) precomplexation is highly unlikely.

As illustrated in Figure 4, the metalation of hydrazone **6** by LDA in hexane with added TMEDA is readily monitored by following the loss of the absorbance at 1636 cm^{-1} corresponding to hydrazone **6** and the appearance of the absorbance at 1570 cm^{-1} corresponding to lithiated hydrazone **8**. At the reduced hydrazone concentrations of the kinetic analysis, an absorbance tentatively attributed to an LDA–lithiated hydrazone mixed aggregate (**9**) is also observed as a shoulder at 1560 cm^{-1}.[15] Unfortunately, the poor NMR spectroscopic properties of lithiated hydrazones continue[3] to preclude rigorous structure determination of either **8** or **9**.

Hydrazone Metalation Kinetics. General. The kinetics of metalation of **6** were studied at 20.0 ± 0.1 °C by using the continuous flow apparatus described previously.[3] The LDA was generated from diisopropylamine and *n*-BuLi and multiply recrystallized.[4] Pseudo-first-order conditions were established with LDA at normal concentrations (typically 0.13 M) by restricting the hydrazone concentration to 0.004 M. The TMEDA was maintained at high, yet adjustable, concentrations (in THF or hexane cosolvent) to determine the mathematical form of the TMEDA dependence. As a result of the delicately balanced **8**/**9** equilibrium, monitoring the formation of either **8** or **9** leads to small spurious effects on the measured pseudo-first-order rate constants. Monitoring the less intense absorbance of starting material at 1636 cm^{-1} affords numerically comparable results, superior nonlinear least-squares analyses, and a greater reproducibility.[16] Improvements resulting from automated data collection and other minor adjustments to the previous protocol are described in the Experimental Section.

Hydrazone Metalation Kinetics. Order in Hydrazone. The metalation of **6** in THF/TMEDA follows clean first-order behavior in **6** to well beyond six half-lives; Figure 5 depicts a representative data set. Random scatter in the raw data is greater than that previously observed in neat THF and shows a proportionality to the TMEDA concentration. After completion of >98% of the kinetics described herein the scatter was traced to N_2 degassing in the flow system. Using helium as the inert atmosphere eliminated the scatter without measurably influencing the rate constants.

In principle, low concentrations of mixed aggregate, homonuclear aggregate, or any unseen byproduct of the reaction (such as diisopropylamine[17] or TMEDA metalation products[18,19]) could measurably influence the rate of the metalation. Very simple control experiments excluded all spurious rate effects. Upon completion of a number of the kinetic runs, the spectral baseline was reestablished, an additional aliquot of **6** was added, and the pseudo-first-order rate constant for the disappearance of **6** was determined. Differences in the measured rate constants for the first and second aliquots were always equal within experimental error (±10%).

Hydrazone Metalation Kinetics. Kinetic Isotope Effects. Comparison of the metalation rates of **6** and **6**-d_3 in neat TMEDA reveal an isotope effect (k_H/k_D = 8.3 ± 1.2) consistent with a mechanism involving rate-determining proton transfer.

6-d_3

Hydrazone Metalation Kinetics. Dependence on TMEDA Concentration. Figure 6 illustrates the dependence of the pseudo-first-order rate constants on the TMEDA concentration with THF as a cosolvent.[20] There are two striking conclusions to be drawn from these data: The metalation rate is independent of the mole fraction of TMEDA, and the rates of hydrazone met-

(14) For leading references to detectable organolithium–substrate precomplexation, see: Klumpp, G. W. *Recl. Trav. Chim.* **1986**, *105*, 1.

(15) Addition of a solution of LDA in TMEDA to lithiated hydrazone **8** pushes the equilibrium toward mixed aggregate **9** as evidenced by the appearance of a shoulder at 1560 cm^{-1} at the expense of the absorbance at 1570 cm^{-1}.

(16) Monitoring formation of product afforded rate constants that were within 20% of the values determined by loss of starting material over most TMEDA concentrations. However, the magnitude of the random scatter was greater by approximately a factor of 3 and a 30% decrease in the measured rate constant occurred from 95% TMEDA/THF to neat TMEDA. Whether this more accurately reflects the absolute rate in neat TMEDA is not of immediate importance to the mechanistic conclusions.

(17) Spectroscopic studies reveal that diisopropylamine does not measurably bind to LDA in hexane at −95 or 20 °C.

(18) Solvent decomposition by lithium amides occurs slowly at ambient temperatures (ref 36). Furthermore, the metalation of TMEDA (ref 19) appears to be mediated by LDA at 20 °C as evidenced by a very slow growth of an absorbance at 1545 cm^{-1}.

(19) Melchior, M. T.; Klemann, L. P.; Whitney, T. A.; Langer, A. W., Jr. *Am. Chem. Soc., Polym. Prepr.* **1972**, *13*, 649. Koehler, F. H.; Hertkorn, N.; Bluemel, J. *Chem. Ber.* **1987**, *120*, 2081.

(20) The absolute values for the rate constants in neat THF are 30% lower than measured previously (ref 3) due to changes in the data processing described in the Experimental Section.

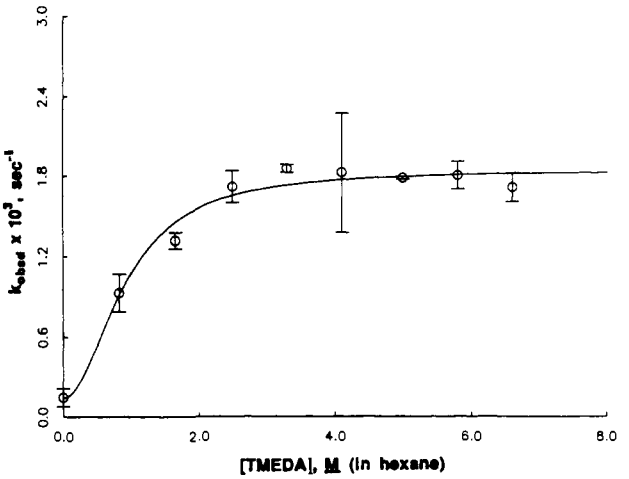

Figure 7. Plot of k_{obsd} versus [TMEDA] in hexane cosolvent for the metalation of hydrazone **6** (0.004 M) by LDA (0.13 M) at 20.0 ± 0.1 °C. The error bars correspond to ± one standard deviation (σ) calculated from triplicate runs. The curve depicts the result of a nonlinear least-squares fit to the expression in eq 11 weighted to $1/\sigma^2$.

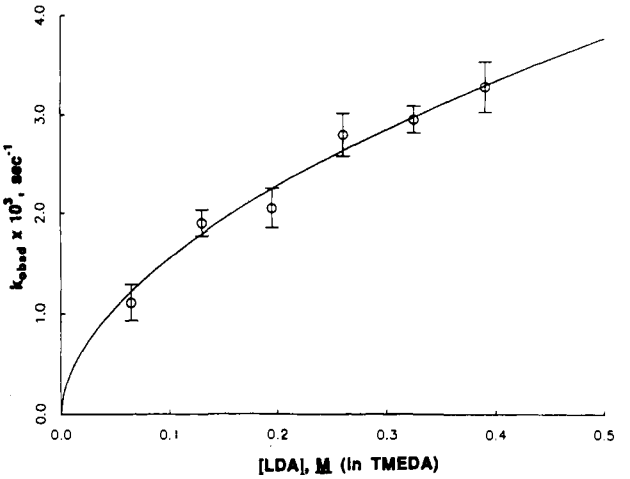

Figure 8. Plot of k_{obsd} versus [LDA] in TMEDA for the metalation of hydrazone **6** (0.004 M) at 20.0 ± 0.1 °C. The error bars correspond to ± one standard deviation (σ) calculated from triplicate runs. The curve depicts the result of a linear least-squares fit to eq 6 weighted to $1/\sigma^2$.

alation by the LDA–THF and LDA–TMEDA solvates (corresponding to the left-hand and right-hand y-intercepts of Figure 6) are indistinguishable (±10%). The coincidental reaction rates in neat THF and neat TMEDA are especially surprising considering their dramatically different affinities toward LDA (see above). Unfortunately, the equivalent metalation rates remove any opportunity to kinetically monitor the substitution of TMEDA for THF within the lithium coordination sphere of LDA. (If the metalation rates had been different, a quantifiable sigmoidal function might have been discernible.[21])

The dependence of the pseudo-first-order rate constants on TMEDA concentration with hexane as the cosolvent proves to be especially revealing (Figure 7). LDA in pure hexane shows a low (but measurable) reactivity toward metalation of **6**. The rate constants measured as a function of TMEDA concentration show saturation behavior, with leveling-off observable at high (>25% *by volume*) TMEDA concentrations. (As a comparison, the spectroscopic and rate data of LDA in THF–hexane mixtures show saturation behavior with less than 2.0 molar equiv of added THF per lithium.[3]) The spectroscopic studies show that *the saturation behavior is the result of the coordination of TMEDA to the intact dimer structure rather than a result of monomer formation.* In fact, the saturation kinetics correlates quantitatively with the LDA solvation equilibrium measured spectroscopically (see below).

***N,N*-Dimethylhydrazone Metalation Kinetics. Dependence on LDA Concentration.** Figure 8 illustrates the dependence of the pseudo-first-order metalation rate constants on the LDA concentration (0.065–0.39 M) in neat TMEDA. A weighted, nonlinear least-squares fit to the general expression in eq 4 provides a calculated LDA order, n, of 0.55 ± 0.05. This LDA order is consistent with a spectroscopically invisible dimer–monomer preequilibrium. We can now complete the general mechanistic scenario outlined by eqs 5–8. Although there is no analytical

$$k_{obs} = k'[\mathrm{LDA}]^n \quad (4)$$

$$(\mathrm{LDA})_x + \mathrm{TMEDA} \overset{k_{eq}[\mathrm{TMEDA}]}{\rightleftharpoons} (\mathrm{LDA{\cdot}TMEDA})_2 \quad (x = 2, 3, 4, \ldots) \quad (5)$$

$$\tfrac{1}{2}(\mathrm{LDA{\cdot}TMEDA})_2 + \mathbf{6} \overset{k_1/k_{-1}}{\rightleftharpoons} \mathrm{LDA{\cdot}TMEDA{\cdot}}\mathbf{6} \quad (6)$$

$$(\mathrm{LDA})_x + \mathbf{6} \xrightarrow{k_2} \mathbf{8/9} \quad (7)$$

$$\mathrm{LDA{\cdot}TMEDA{\cdot}}\mathbf{6} \xrightarrow{k_3} \mathbf{8/9} \quad (8)$$

rate equation due to the uncertainty in the mechanism of metalation by unsolvated LDA (eq 7), the expression in eq 9 represents a reasonable approximation. The constant, C, is appended to

$$d[\mathbf{6}]/dt = \{k_3 K_{eq}^{1/2}[\mathbf{6}](k_1/k_{-1})[(\mathrm{LDA})_2]^{1/2}[\mathrm{TMEDA}]\}/(1 + K_{eq}^{1/2}[\mathrm{TMEDA}]) + C \quad (9)$$

reflect the minor contribution of solvent-free LDA to the metalation rate (eq 7) and to define the y-intercept. (Although this contribution would not formally be constant, the value is of a magnitude comparable to experimental error.) In the limit of high TMEDA concentration, the rate equation simplifies to the form of eq 10, showing consistency with the reaction orders in TMEDA, LDA, and hydrazone. The metalation rates conform to the rate

$$d[\mathbf{6}]/dt = (k_1/k_{-1})k_3[(\mathrm{LDA})_2]^{1/2}[\mathbf{6}] \quad (10)$$

expression described by eq 9 (curve in Figure 7). The calculated value of K_{eq} = 1.2 ± 0.3 agrees well with the value of 1.3 ± 0.3 determined independently from the spectroscopic studies at 20 °C.

Structure and Reactivity of LDA–Dimethylethylamine Solvates. Before we could seriously consider structural details for hydrazone metalation, we required additional information concerning the TMEDA–LDA interaction. We were troubled by the inferior solvating capabilities of TMEDA relative to THF. Also, the rate equations determined in THF and TMEDA are completely analogous despite the profound difference in solvent structure. Both observations seemed incompatible with the notion that TMEDA functions as a bidentate ligand. Accordingly, we completed our studies of the solvent dependence with a cursory investigation of the structure and reactivity of LDA in dimethylethylamine (DMEA). Our premise was simple: If TMEDA binds in an η^1 (nonchelating) rather than η^2 (chelating) fashion, then the spectroscopic and kinetic profiles of LDA–DMEA and LDA–TMEDA should exhibit strong parallels, including related saturation behavior.

NMR spectra of [^{6}Li,^{15}N]LDA in neat DMEA at −55 °C show a ^{6}Li triplet (δ 2.18 ppm, J_{Li-N} = 5.2 Hz) and ^{15}N quintet (δ 73.3 ppm, J_{Li-N} = 4.9 Hz)[22] consistent with dimer **10**. Treatment of solvent-free [^{6}Li]LDA in hexane with 1.0 equiv of DMEA at −95 °C results in almost complete conversion to dimer **10**. Spectra recorded at elevated probe temperatures reveal the envelope of ^{6}Li resonances characteristic of unsolvated LDA, indicating a strongly temperature-dependent desolvation. Monitoring the solvated and unsolvated forms of LDA as a function of [DMEA] in hexane at 20 °C reveals equivalent capacities of TMEDA and DMEA to solvate LDA; identical values of K_{eq} (1.3 ± 0.3) are obtained from nonlinear least-squares fits of the TMEDA and DMEA NMR spectroscopic data (Figures 3 and 9) to eq 3.[23]

(21) Depue, J. S.; Collum, D. B. *J. Am. Chem. Soc.* **1988**, *110*, 5524.

Scheme II

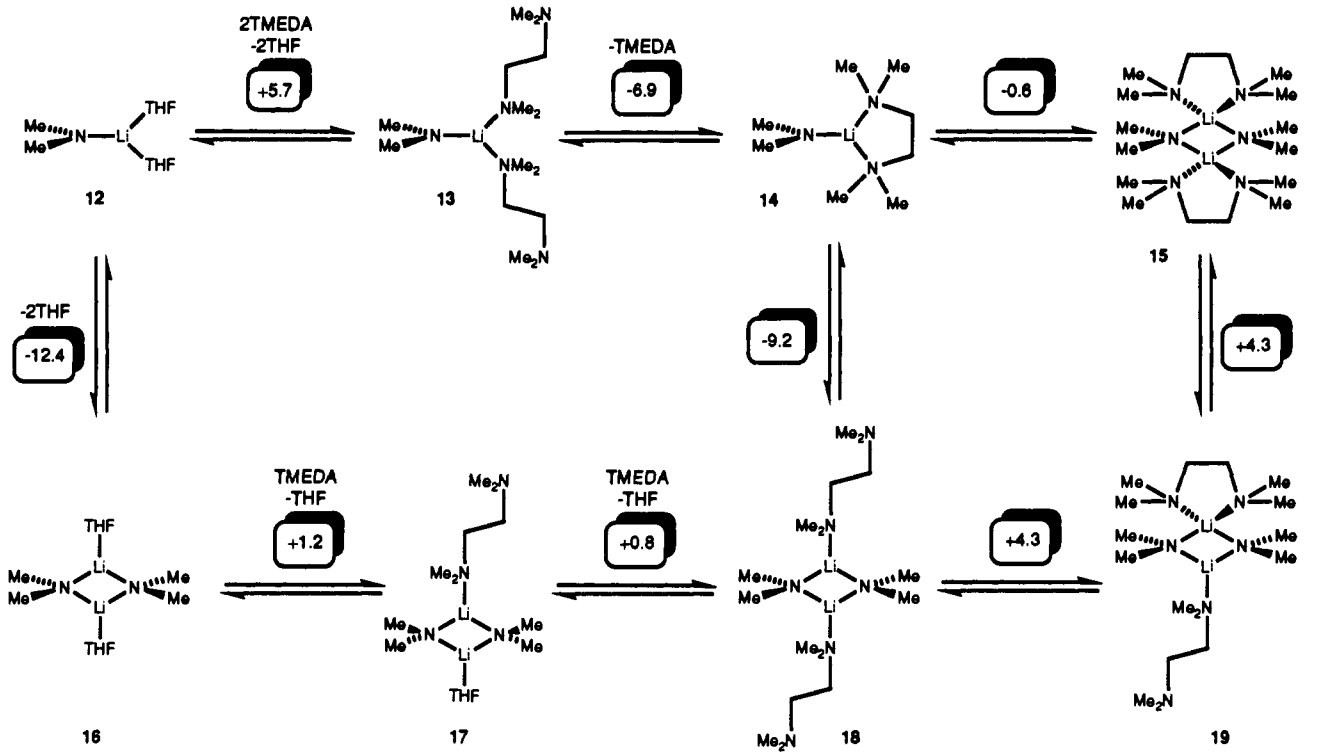

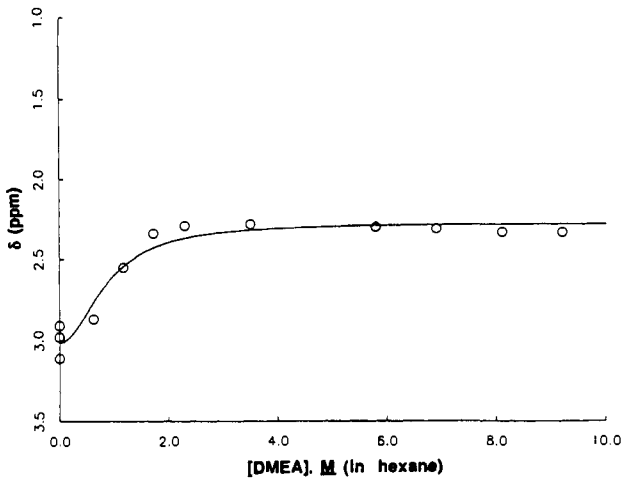

Figure 9. Statistically weighted and averaged ^{6}Li chemical shifts[22] measured at 20 °C on 0.13 M solutions of [^{6}Li]LDA in hexane containing varying concentrations of added DMEA.

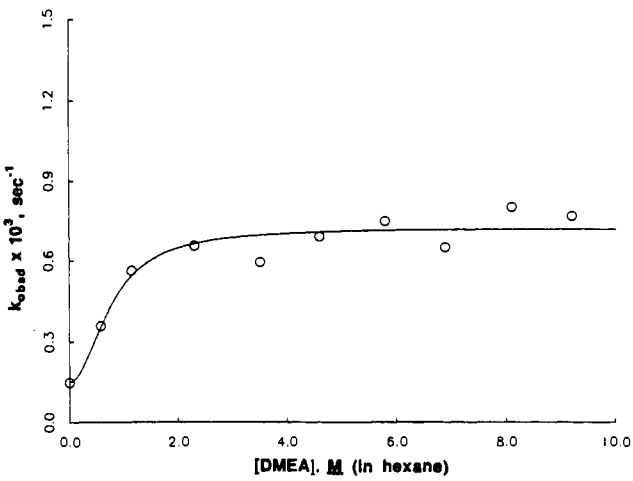

Figure 10. Plot of k_{obsd} versus [DMEA] in hexane cosolvent for the metalation of hydrazone **6** (0.004 M) by LDA (0.13 M) at 20.0 ± 0.1 °C. The curve depicts the result of a nonweighted linear least-squares fit to eq 6.

Similarly, the solvent dependencies for metalation of hydrazone **6** in TMEDA/hexane and DMEA/hexane mixtures (Figures 7 and 10) show comparable saturation behavior.[24] Moreover, the dependence of the pseudo-first-order rate constant on the [LDA] determined over a 10-fold concentration range in neat DMEA reveals a 0.49 ± 0.02 order. The kinetic and spectroscopic comparisons lead to the conclusion that intermediates and transition structures bearing the chelated TMEDA substructure (**2**) are of little consequence during the metalation. We do note, however, that LDA is more fluctional in TMEDA than in DMEA. Whereas the ^{6}Li resonance of the TMEDA-solvated dimer displays ^{6}Li–^{15}N coupling only below −40 °C, coupling in the analogous DMEA-solvated dimer can be observed at 25 °C. Possibly chelated monomer **11** is an important determinant of the subunit exchange rates in TMEDA.[13]

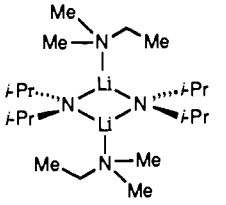

10

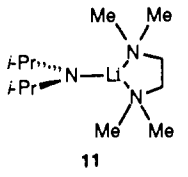

11

MNDO Calculations. We recently completed extensive MNDO computational studies of various aggregates of Me_2NLi, LDA, and lithium 2,2,6,6-tetramethylpiperidide (LiTMP) solvated by

(22) A resonance corresponding to DMEA at natural ^{15}N abundance appears at 25.7 ppm.

(23) The solvated and unsolvated forms of LDA in DMEA/hexane mixtures readily resolve by ^{6}Li NMR spectroscopy at 20 °C. The average chemical shifts used in Figure 10 derive from peak integrations with proper statistical weighting.

(24) Nonlinear least-squares fit to eq 9 (as described in the text for TMEDA) afforded K_{eq}(DMEA) = 1.7 ± 0.5.

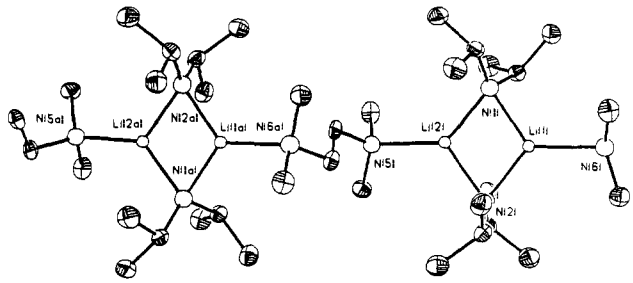

Figure 11. Perspective view of $[(LDA)_2TMEDA]_\infty$. The figure depicts only one $(LDA)_2TMEDA$ segment with appended TMEDA fragments and represents only one-half of the crystallographically asymmetric unit. The material crystallizes with two very nearly identical fragments in the asymmetric unit. Further details are provided in the supplementary material.

H_2O, Me_2O, THF, $(H_2N)_3P{=}O$, and $(Me_2N)_3P{=}O$ (HMPA).[5] MNDO calculations reproduced the experimentally determined aggregation and solvation states quite well, although possible exaggeration of steric effects was evident. Of special note, however, is that minima (albeit high energy) bearing reasonable geometries could be located even in the most sterically congested systems.

The results for solvation of Me_2NLi by THF and TMEDA are summarized in Scheme II. The enthalpies depicted in boxes above the equilibrium arrows are normalized to a per-lithium basis.[25] The relatively unhindered Me_2NLi fragment leads to a number of interesting conclusions: (1) The most stable dimer **18** is predicted to be more stable than monomers whether TMEDA functions as a chelating (η^2) or nonchelating (η^1) ligand. (2) Displacement of TMEDA by THF on the dimer is favorable irrespective of the binding mode of the TMEDA. Moreover, TMEDA chelation on the dimer is highly destabilizing relative to the η^1 binding mode. (3) The most stable monomer is suggested to be the TMEDA-chelated monomer **14**. In contrast, a comparison of $MeLi(\eta^2\text{-TMEDA})$ with $MeLi(NMe_3)_2$ suggests the chelate effect to be deleterious both enthalpically and entropically.[26] (4) As a consequence of the *instability* of TMEDA-solvated dimer **18** relative to THF-solvated dimer **16** and the *stability* of TMEDA-solvated monomer **14** relative to THF-solvated monomer **12**, one would expect a greater proportion of monomer in TMEDA than in THF. In this context, the increased fluctionality of LDA in neat TMEDA relative to either neat DMEA or neat THF[3] is consistent with prediction. (5) As a consequence of (2) and (4), TMEDA is predicted to impact on the relative concentrations of monomeric and dimeric Me_2NLi *only* in the absence of THF.

The results of MNDO calculations of various solvated LDA structures are summarized in Scheme III. The enthalpy changes are listed in the boxes and reported as (kcal/mol)/Li. Exhaustive investigation of the dimers revealed no minima bearing chelated TMEDA ligands. Second, dimer **4** bearing two nonchelated TMEDA ligands failed to converge; the enthalpy was determined by fixing the two TMEDA N–Li bond lengths to the optimized value of 2.70 Å found in the monosolvate **23**. Although use of ethylenediamine as a model for TMEDA could provide stable minima, the omission of the methyl groups removes what may be the dominant destabilizing interactions.[27] Furthermore, our experimental results are not in direct conflict with the calculated structures. Thus, we choose to rely on the full calculations as they stand. The notable predictions of MNDO are as follows. Although the chelated monomer **11** is now found to be more stable than the nonchelated dimer **4**, the monosolvated dimer **23** is predicted to be the most stable structure. (The corresponding $(Me_2NLi)_2(\eta^1\text{-TMEDA})$ is 3.0 (kcal/mol)/Li less stable than disolvate **18**.) While the spectroscopic data described above do not provide a distinction of **4** and **23**, the zero-order TMEDA dependence found in the hydrazone metalation argues against **23** as the observable form. The steric demands of the LDA–TMEDA solvates are manifested by highly exothermic displacement of TMEDA by THF. As seen for Me_2NLi, the calculations suggest that deaggregation is more favorable in TMEDA than in THF by virtue of a disproportionate destabilization of the TMEDA-solvated dimer rather than inordinate monomer stabilization.

Overall, the MNDO calculations corroborate the experimental findings showing that TMEDA (1) does not measurably deag-

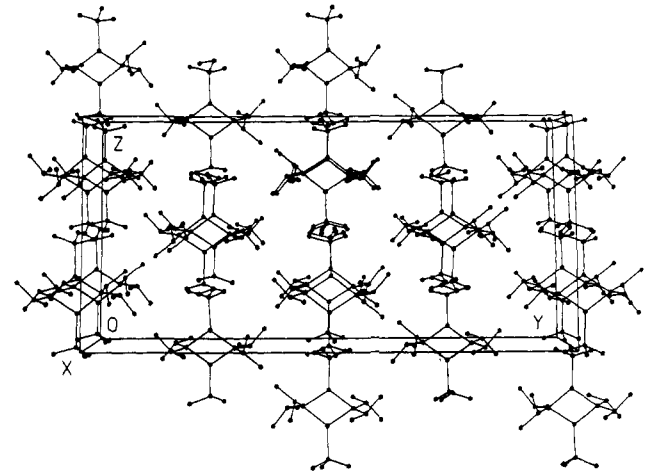

Figure 12. Packing diagram of $[(LDA)_2TMEDA]_\infty$.

Table II. Crystallographic Data for the LDA/TMEDA Complex

molec formula	$[(C_6H_{14}NLi)_2{\cdot}(C_6H_{16}N_2)]_2$
formula wt	661.07
cryst system	monoclinic
space group	$P2_1/c$
a, Å	9.018 (5)
b, Å	31.898 (13)
c, Å	15.917 (9)
α, deg	90.00
β, deg	99.44 (4)
γ, deg	90.00
no. of orientation reflns; 2θ range, deg	25; 24–26
V, Å^3	4517 (1)
Z	4
D_{calcd}, g/cm^3	0.97
μ(Mo Kα radiatn λ = 0.71069), cm^{-1}	0.5
temp, °C	~−80
cryst dimens	not measd
scan type	θ:2θ
scan range, deg	$3.5 < 2\theta < 45$
total no. of reflns ($+h,+k,\pm l$) recorded	6736
no. of nonequiv reflns recorded	6355
R_{merge} (on I)	0.019
no. of reflns retained [$I > 3.0\sigma(I)$]	4274
no. of params refined	433
R (R_w)	0.072 (0.073)
goodness-of-fit	2.60

Selected Structural Parameters for the LDA/TMEDA Aggregate Depicted in Figure 11[a]

bond or angle	Å or deg	N_{obs}	std dev
Li–N(LDA)	2.017	8	0.014
Li–N(TMEDA)	2.163	4	0.026
Li–N(LDA)–Li	72.9	4	0.2
N(LDA)–Li–N(LDA)	107.0	4	0.9
out-of-plane deviatn of Li atom (from plane of three attached Ns)	0.061	4	0.03

[a] Note that these values are averages of the structurally equivalent but crystallographically independent parameters.

(25) The calculated absolute heats of formation for the compounds in Schemes II and III are as follows: TMEDA, +5.6; THF, −59.3; **4**, −58.2; **11**, −32.6; **12**, −145.2; **13**, −9.6; **14**, −22.2; **15**, −45.6; **16**, −196.6; **17**, −129.3; **18**, −62.8; **19**, −54.1; **20**, −157.7; **21**, −17.0; **22**, −206.1; **23**, −75.9. The value of TMEDA is adjusted from a literature value of +7.7 (ref 26).

(26) Kaufmann, E.; Gose, J.; Schleyer, P. v. R. *Organometallics* **1989**, *8*, 2577.

(27) For a discussion of the cone angle of trialkylamines in the context of transition-metal ligation, see: Seligson, A. L.; Trogler, W. C. *J. Am. Chem. Soc.* **1991**, *113*, 2520.

Scheme III

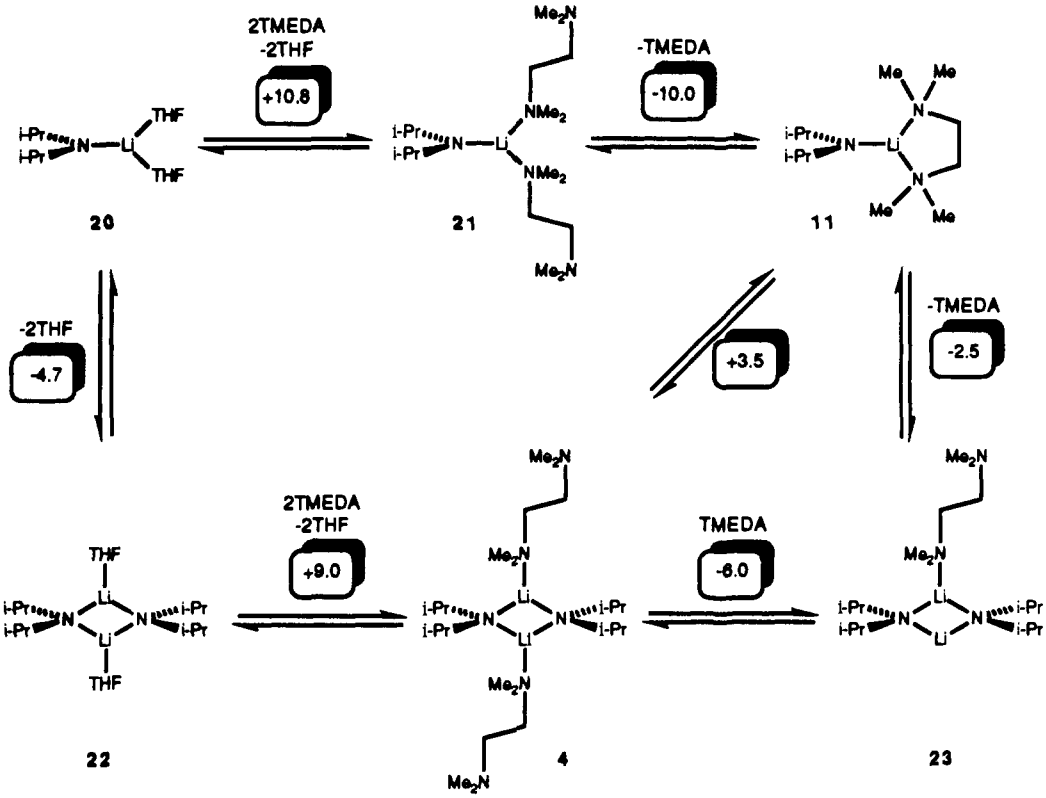

gregate lithium amides, (2) does not readily bind dimeric amides in a bidentate fashion, and (3) cannot compete with THF for coordination of LDA.

X-ray Crystal Structure of $[(LDA)_2TMEDA]_\infty$. From a solution of LDA–TMEDA in hexanes it was possible to obtain crystals of stoichiometry $(LDA)_2TMEDA$. A computer-generated plot of the X-ray crystal structure is depicted in Figure 11. In this structure, the TMEDA adopts an extended, staggered conformation and bridges two dimeric LDA units. The net result is formation of infinite chains of TMEDA-linked dimeric units stacked in layers as depicted in Figure 12. Hence, we find that in the solid state the Li atoms prefer to be planar tricoordinate and the TMEDA ligands neither chelate to Li nor deaggregate the LDA dimer substructure. Table II lists some of the characteristic distances and angles along with some of the relevant crystallographic parameters obtained for this structure. It is interesting that crystals of unsolvated LDA showing a helical polymer structure were also generated in the presence of TMEDA.[28]

Discussion

Summary. ^6Li, ^{13}C, and ^{15}N NMR spectroscopic studies of [^6Li,^{15}N]LDA demonstrate that LDA in hexane is readily solvated by TMEDA at −100 °C to provide a dimer but does not deaggregate to monomer even in neat TMEDA. TMEDA binds reluctantly to LDA at ambient temperature even in the absence of any other donor ligands; TMEDA concentrations in excess of 25% by volume (in hexane) are required to fully occupy the available coordination sites of dimeric LDA. In contrast, THF shows a high affinity for LDA at both low and ambient temperatures. Studies of LDA in dimethylethylamine (DMEA) reveal spectroscopic behavior analogous to TMEDA despite the lack of a potentially chelating functionality on the DMEA. We conclude that the stable LDA structure in neat TMEDA solution is the nonchelated, disolvated dimer **4** rather than the anticipated doubly chelated dimer **5**. The resistance of TMEDA to form chelate **5** is also manifested in an X-ray crystal structure showing an infinite array of dimer units connected by η^1 TMEDA linkages (Figures 11 and 12).

MNDO studies of Me_2NLi and LDA are in strong agreement with the experimental results. Dimeric amides display dramatically lower affinities for TMEDA than THF and no tendency whatsoever to form chelated (η^2) TMEDA solvates. The most stable TMEDA solvates are the η^1 solvates **18** and **23**. Although the spectroscopic studies do not rigorously exclude **23** as the observable form, the zero-order TMEDA dependence in the hydrazone metalation argues strongly against it. MNDO predicts an increased propensity of lithium amides to deaggregate in the presence of only TMEDA (no added THF) due to a combination of monomer stabilization and dimer destabilization. Monomers appear to derive stabilization from the chelate effect but remain unstable relative to dimers.

Rate studies of hydrazone metalation are consistent with the sequence delineated in eqs 5–8. We describe the mechanism with inclusion of postulated intermediates as outlined in Scheme I. A substantial kinetic isotope effect, a first-order rate dependence on hydrazone concentration, and a $^1/_2$-order rate dependence on the LDA concentration[3,29] are fully consistent with a spectroscopically invisible deaggregation preequilibrium followed by a rate-determining proton transfer. IR and NMR spectroscopic evidence indicate that an LDA–TMEDA–hydrazone complex such as **7**, while likely to be of mechanistic significance,[14,30] does not build up to appreciable concentrations at ambient temperatures. The dependence of the hydrazone metalation rate on the TMEDA concentration (in hexane) displays saturation behavior that quantitatively correlates with the spectroscopically detected solvation of the LDA dimer unit. The spectroscopic and rate data for LDA/TMEDA, LDA/DMEA, and LDA/THF[3] lead us to conclude that the metalation of **6** by LDA proceeds through intermediates (and transition states) that are essentially isostructural (Scheme I). The TMEDA–DMEA comparison lends strong support to the contention that TMEDA chelates play little

(28) Barnett, N. D. R.; Mulvey, R. E.; Clegg, W.; O'Neil, P. A. *J. Am. Chem. Soc.* **1991**, *113*, 8187.

(29) Newcomb, M.; Varick, T. R.; Goh, S.-H. *J. Am. Chem. Soc.* **1990**, *112*, 5186.

(30) Bachrach, S. M.; Ritchie, J. P. *J. Am. Chem. Soc.* **1989**, *111*, 3134 and references cited therein.

if any role along the reaction coordinate. The depiction of intermediate 7 as a π complex is a speculative suggestion based on regiochemical studies of hydrazone metalation[31] and the often cited tendency of lithium to achieve approximate tetrahedral coordination when sterically possible.[32]

The indistinguishable rate constants for metalation of **6** in neat THF and neat TMEDA are initially surprising given that THF has a >20-fold increased affinity for dimeric LDA. We are reminded that it is the relative (not the absolute) free energies of the ground state and transition state that determine the observed metalation rate. A less obvious consequence is that there is no correlation between the strength of the solvent–lithium interaction in the ground state and the hydrazone metalation rate.

On the Role of TMEDA in the Chemistry of Lithium Amides. There exists limited evidence that TMEDA influences the chemistry of lithium amides. Several papers describe modest effects of TMEDA on the structure[33,34] or reactivity[35] of lithium amides (possibly within experimental error), and others report no effect of TMEDA at all.[36] For the most part, however, the reasons for adding TMEDA to solutions of lithium amides remain undisclosed.[37,38] Even when a change in reactivity or selectivity can be detected upon addition of TMEDA, uncontrolled variables cloud the mechanistic interpretation. For example, Rathke and co-workers found that TMEDA influences the stereochemistry of ketone enolization by lithium 2,2,6,6-tetramethylpiperidide (LiTMP) in THF.[39] Curiously, the effects of added TMEDA are attenuated considerably if the enolization proceeds to low percent conversions (i.e., [LiTMP]/[ketone] > 4). However, LiTMP-mediated enolizations are hypersensitive to the influence of mixed aggregation—effects that are manifested by changes in selectivity with percent conversion.[40,41] Thus, it is possible that TMEDA influences the mixed aggregation equilibria (and, in turn, the stereochemistry of ketone enolization) without coordinating to the hindered lithium amide fragment.

Fraser and Mansour reported the only instance that we are aware of where TMEDA strongly influences the chemistry of lithium amides.[42] They found that addition of 1.0 equiv of TMEDA to solutions of LDA in THF causes the rate of lithiation of triphenylmethane to increase by a factor of 40 relative to that for LDA in neat THF (eq 11). Although the TMEDA-mediated

$$Ph_3C\text{–}H \xrightarrow[\text{TMEDA}]{\text{LDA/THF}} Ph_3C\text{–}Li \qquad (11)$$

rate acceleration was surprising in light of our demonstration that

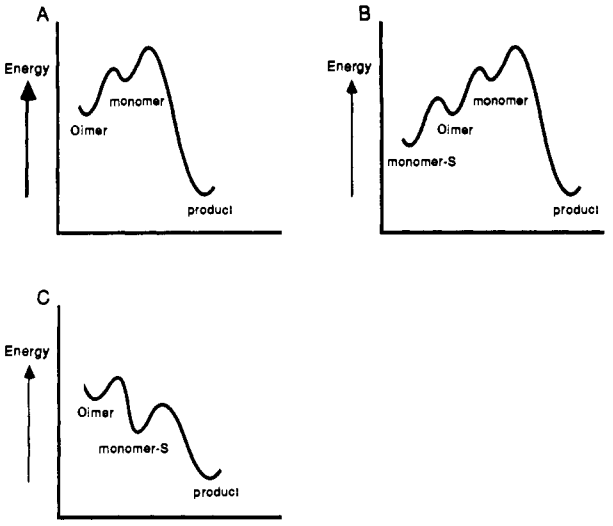

Figure 13.

TMEDA cannot compete with bulk THF for coordination sites on LDA, we repeated the work and confirmed their results.[43] We offer the following explanation of how the lithiation of hydrazone **6** and Ph_3CH under almost identical conditions could exhibit such disparate dependencies on added TMEDA. If an additive such as TMEDA coordinates to both the ground state and transition state, the two solvation energies will tend to cancel; there will not necessarily be a correlation between metal–ligand bond strength and observed reaction rates. This appears to be the case for the metalation of hydrazone **6**, where the substrate provides the additional solvation energy required to effect dimer-to-monomer deaggregation en route to the transition state. On the other hand, if the transition state must attain a higher solvation number than the ground state, highly solvent-dependent rates should be observable. The metalation of Ph_3CH may be an excellent case in point. Since the substrate lacks obvious capacity to precoordinate to the LDA, all solvation energy required to effect a (presumed) dimer deaggregation must come from additional lithium–donor solvent interactions. Any capacity TMEDA has to function as a bidentate ligand could become advantageous by reaction via monomer **11** and transition structure **24** bearing higher formal solvation numbers (per Li) than the ground-state dimer.

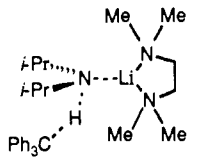

24

Moreover, the metalation of Ph_3CH by LDA is an optimal reaction for observing catalysis by TMEDA since ground-state stabilization will not attenuate the reaction rate—TMEDA does not bind to LDA in the ground state in the presence of THF.

This leads us to an important point. While it may be logical that lower aggregates are more reactive, the correlation of aggregation state and organolithium reactivity is based more on consensus than experiment. The relative reactivities of different aggregation states have been directly determined on only several occasions.[21,44] In cases where fractional organolithium rate dependencies provide support for the intervention of highly reactive lower aggregates,[45] the *transient* lower aggregates are relatively

(31) Ludwig, J. W.; Newcomb, M.; Bergbreiter, D. E. *J. Org. Chem.* **1980**, *45*, 4666.
(32) Wardell, J. L. In *Comprehensive Organometallic Chemistry*; Wilkinson, G., Stone, F. G. A., Abels, F. W., Eds.; Pergamon: New York, 1982. *Ions and Ion Pairs in Organic Reactions*; Szwarc, M., Ed.; Wiley: New York, 1972; Vols. 1 and 2.
(33) Jackman, L. M.; Scarmoutzos, L. M. *J. Am. Chem. Soc.* **1987**, *109*, 5348. Gregory, K.; Bremer, M.; Bauer, W.; Schleyer, P. v. R. *Organometallics* **1990**, *9*, 1485.
(34) Aylett, B. J.; Liaw, C.-F. *J. Organomet. Chem.* **1987**, *325*, 91.
(35) Fraser, R. R.; Akiyama, R.; Banville, J. *Tetrahedron Lett.* **1979**, *20*, 3929. Posner, G. H.; Lentz, C. M. *J. Am. Chem. Soc.* **1979**, *101*, 934. Olofson, R. A.; Dougherty, C. M. *J. Am. Chem. Soc.* **1973**, *95*, 581.
(36) Moss, R. J.; Rickborn, B. *J. Org. Chem.* **1986**, *51*, 1992. Kopka, I. E.; Fataftah, Z. A.; Rathke, M. W. *J. Org. Chem.* **1987**, *52*, 448. Kopka, I. E.; Nowak, M. A.; Rathke, M. W. *Synth. Commun.* **1986**, *16*, 27. Enders, D. In *Asymmetric Synthesis*; Morrison, J. D., Ed.; Vol. 3, p 275. See also ref 39.
(37) Enders, D.; Demir, A. S.; Puff, H.; Franken, S. *Tetrahedron Lett.* **1987**, *28*, 3795. Harris, T. D.; Neuschwander, B.; Boekelheide, V. *J. Org. Chem.* **1978**, *43*, 727. Hoppe, I.; Hoppe, D.; Herbst-Irmer, R.; Egert, E. *Tetrahedron Lett.* **1990**, *31*, 6859. Pez, G.; Galle, J. E. *Pure Appl. Chem.* **1985**, *57*, 1917. Binger, P.; Müller, P.; Wenz, R.; Mynott, R. *Angew. Chem., Int. Ed. Engl.* **1990**, *29*, 1037.
(38) Veracini, S.; Gau, G. *Nouv. J. Chim.* **1978**, *2*, 523.
(39) Fataftah, Z. A.; Kopka, I. E.; Rathke, M. W. *J. Am. Chem. Soc.* **1980**, *102*, 3959. See also: Ireland, R. E.; Wipf, P.; Armstrong, J. D., III *J. Org. Chem.* **1991**, *56*, 650.
(40) Hall, P. L.; Gilchrist, J. H.; Collum, D. B. *J. Am. Chem. Soc.* **1991**, *113*, 9571.
(41) For an excellent review describing the impact of aggregation and mixed aggregation on organolithium structure and reactivity see ref 2e.
(42) Fraser, R. R.; Mansour, T. S. *Tetrahedron Lett.* **1986**, *27*, 331.
(43) In contrast to the literature report (ref 42) in which ^{13}C NMR spectroscopy was used to measure the Ph_3CH metalation half-life, we find that addition of 1 equiv of TMEDA causes a 10-fold rate increase from FT-IR and ^1H NMR spectroscopic data.
(44) McGarrity, J. F.; Ogle, C. A.; Brich, Z.; Loosli, H.-R. *J. Am. Chem. Soc.* **1985**, *107*, 1810. Jackman, L. M.; Dunne, T. S. *J. Am. Chem. Soc.* **1985**, *107*, 2805. Jackman, L. M.; Rakiewicz, E. F.; Benesi, A. J. *J. Am. Chem. Soc.* **1991**, *113*, 4101 and references cited therein.

Scheme IV

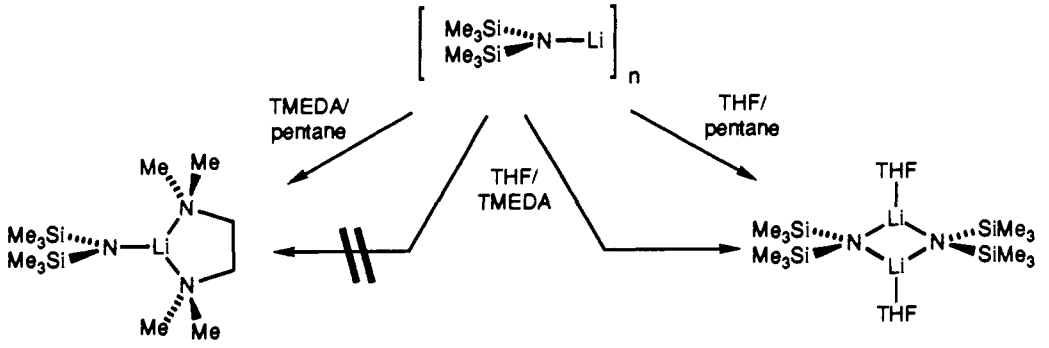

25

unstable *by definition*. We cited limited spectroscopic evidence that chelated monomer **11** may be a key intermediate in the subunit exchange between observable dimers. In the hypothetical event that added TMEDA had caused **11** to become an observable species, would metalation rates increase? If new reaction pathways are not made accessible then *formation of the new monomer would represent an unproductive side-equilibrium, promoting a rate retardation according to the Principle of Detailed Balance* (compare parts A and B of Figure 13).[46] If monomer **11** and a monomeric transition structure (e.g., **24**) are both stabilized relative to dimer **4** and if monomer **11** becomes an observable form, then a reaction rate increase would be plausible (but not mandated; Figure 13C). One should not forget, however, that *any stabilization of the ground state serves to retard the reaction rate*. Even if a reaction must proceed via a lower aggregate, forcing the deaggregation will not necessarily cause a rate acceleration. In fact, the ideal solvent would be one showing no affinity whatsoever for the ground state and a high affinity for the transition state. The metalation of hydrazones provides an interesting illustration of the point. The stability of **11** has no bearing on the transition-state stability since the evidence points to a transition state with an η^1-coordinated TMEDA ligand. Observable formation of **11** would indeed represent an unproductive side-equilibrium, causing a rate retardation. Even if a reaction *must* proceed via a lower aggregate, forcing the deaggregation will not cause a rate acceleration *if the observable lower aggregate is at the wrong (higher) solvation number*.

One might ask whether observable deaggregation necessarily implicates high stabilization conferred by solvation. Recent studies of lithium hexamethyldisilazide (LiHMDS) demonstrate that TMEDA-mediated deaggregation does not constitute evidence of an inordinately strong metal–ligand interaction (Scheme IV).[47] LiHMDS was found to be exclusively monomer in the presence of 5.0 equiv of TMEDA and exclusively dimer in the presence of 5.0 equiv of THF. Exclusive formation of the (THF-solvated) dimer in the presence of THF and TMEDA illustrates that TMEDA deaggregates LiHMDS *only in the absence of THF*. In essence, the TMEDA-solvated monomer results from the *instability* of the TMEDA-solvated dimer. In turn, the reactivity of monomer **25** should not be attenuated by excessive stabilization.

We now come to the final rhetorical question: is TMEDA a good ligand for lithium? An extensive survey of the literature failed to afford a simple answer. Since a detailed critique is well beyond the scope of this paper, we will simply note that the structural and mechanistic consequences of TMEDA appear to be highly dependent on steric effects, temperature, and cosolvent. Moreover, much of the lore of organolithium chemistry is based upon the logic that bidentate ligands such as TMEDA influence structure and reactivity through strong metal–ligand interactions. It is important to establish secure mechanistic foundations.

Conclusions. The spectroscopic and kinetic studies described above lead us to the following conclusions:

1. TMEDA is a poor ligand for LDA, affording η^1-solvated dimer **4** as the structure in solution only with a large molar excess of TMEDA. TMEDA cannot compete with even limited concentrations of THF.

2. A solid-state structure determination reveals LDA dimer units linked into infinite chains by η^1-solvated bridging TMEDA ligands.

3. LDA metalates *N,N*-dimethylhydrazones in TMEDA via a mechanism involving a spectroscopically invisible dimer–monomer preequilibrium, followed by rate-limiting proton transfer. Spectroscopic and kinetic comparisons of TMEDA with dimethylethylamine indicate that TMEDA does not function in a chelating capacity at any crucial points along the reaction coordinate.

4. The hydrazone metalation rate shows a zero kinetic order in TMEDA. One consequence is that the reaction rates do not correlate with the solvent affinities for LDA.

5. Contrasting behavior observed for metalations of triphenylmethane by LDA in THF/TMEDA illustrates the mechanistic dependence of kinetic basicity.

Experimental Section

Reagents and Solvents. THF, dimethylethylamine (DMEA), TMEDA, and all hydrocarbons were distilled by vacuum transfer from blue or purple solutions containing sodium benzophenone ketyl. The hydrocarbon stills contained 1% tetraglyme to dissolve the ketyl. ^{6}Li metal (95.5% enriched) was obtained from Oak Ridge National Laboratory. The [^{6}Li]ethyllithium used to prepare the ^{6}Li-labeled LDA was prepared and purified by the standard literature procedure.[4,48] The LDA, [^{6}Li]LDA, and [^{6}Li,^{15}N]LDA used for spectroscopic and kinetic studies were isolated as analytically pure solids as described elsewhere.[4] The diphenylacetic acid used to check solution titers[49] was recrystallized from methanol and sublimed at 120 °C under full vacuum. Air- and moisture-sensitive materials were manipulated under argon or nitrogen by using standard glovebox, vacuum line, and syringe techniques.

NMR Spectroscopic Analyses. Samples for spectroscopic analyses were prepared from isotopically labeled LDA[4] using procedures described in detail elsewhere.[40,50] Similarly, the ^{6}Li, ^{15}N, and ^{13}C NMR spectra were recorded on a Varian XL-400 spectrometer by well-documented procedures.[5] The ^{15}N NMR spectra are referenced to [^{15}N]aniline at −100 °C (52 ppm). The ^{6}Li NMR spectra are referenced to 0.3 M [^{6}Li]LiCl/MeOH at −100 °C (0.0 ppm). Natural abundance DMEA and TMEDA show ^{15}N resonances at 25.7 and 21.3 ppm, respectively.

Kinetics. The apparatus and flow system for following the kinetics of metalation of hydrazone **6** have been described previously.[3] Automated data collection allowed the typical rate constant to be determined from 150–300 independent absorbance measurements (Figure 5). The measured rate constants depend minimally on the choice of frequency to establish the spectral baseline; 1710 cm^{-1} was found to minimize random

(45) Wardell, J. L. In *Comprehensive Organometallic Chemistry*; Wilkinson, G., Stone, F. G. A., Abels, F. W., Eds.; Pergamon: New York, 1982; Vol. 1, Chapter 2.

(46) Casado, J.; Lopez-Quintela, M. A.; Lorenzo-Barral, F. M. *J. Chem. Educ.* **1986**, *63*, 450. Hammes, G. G. *Principles of Chemical Kinetics*; Academic Press: New York, 1978; pp 14–15.

(47) Bernstein, M. P.; Collum, D. B., submitted for publication.

(48) Lewis, H. L.; Brown, T. L. *J. Am. Chem. Soc.* **1970**, *92*, 4664. For a detailed preparation, see ref 4.

(49) Kofron, W. G.; Baclawski, L. M. *J. Org. Chem.* **1976**, *41*, 1879.

(50) Romesberg, F. E.; Gilchrist, J. H.; Harrison, A. T.; Fuller, D. J.; Collum, D. B. *J. Am. Chem. Soc.* **1991**, *113*, 5751.

scatter and give the most reproducible results. All other aspects of the kinetic and statistical analysis were carried out as described previously.[3]

X-ray Crystal Structure Determination of $[(LDA)_2TMEDA]_\infty$. A 40-mL, thick-walled centrifuge tube containing a stir bar, fitted with a septum, flushed with N_2, and cooled to 0 °C was charged sequentially with hexane (2.5 mL), diisopropylamine (1.4 mL), and 2.5 M *n*-BuLi in hexanes (4.0 mL). The resulting syrupy mixture was placed in a −30 °C freezer for 4 h, during which time a white precipitate of LDA formed. Excess solvent was removed via syringe and the precipitate was washed with 2 × 3 mL of fresh hexane by introduction and removal of the solvent with a syringe at 0 °C. The solid was redissolved by adding hexane (2.5 mL) and TMEDA (45 mL) while stirring. The solution was placed in a −40 °C freezer overnight, during which time needle-like crystals and amorphous solid deposited. The vessel was warmed to 0 °C to dissolve the crystals and the remaining undissolved solid was removed by filtration under N_2. The clear solution was placed in a −10 °C freezer overnight, affording substantially improved needle-like crystals. An additional recrystallization at −10 °C over 12 h provided superb crystals.

MNDO Calculations. MNDO[51] calculations were performed on an IBM 3090 supercomputer by using a modified version of the MOPAC[52] program. The lithium parameters were those of Clark and Theil.[53] The current lithium parameters appear to accurately reproduce lithium interactions with nitrogen and oxygen.[26,54] All structures were fully optimized under the more rigorous criteria of the keyword PRECISE with no constraints unless explicitly stated otherwise. The heats of formation result from extensive searches for the global minimum starting from several different initial geometries. Symmetrical structures were reoptimized from distorted geometries to ensure that the symmetry is not a computational artifact. The keyword GEO-OK was used with caution to override the small interatomic distance check. All energies quoted refer only to enthalpy to the exclusion of entropic effects other than those implicit in the parametric scheme.

Acknowledgment. We acknowledge the National Science Foundation Instrumentation Program (CHE 7904825 and PCM 8018643), the National Institutes of Health (RR02002), and IBM for support of the Cornell Nuclear Magnetic Resonance Facility. Both D.B.C. and P.G.W. thank the National Institutes of Health for direct support of this work. The computational studies were conducted at the Cornell National Supercomputer Facility, a resource of the Center for Theory and Simulations in Science and Engineering (Cornell Theory Center), which receives major funding from the National Science Foundation and IBM Corp., with additional support from New York State and members of the Corporate Research Institute. We are especially grateful to Evelyn Goldfield (Cornell), Charles Wilcox (Cornell), Barry Carpenter (Cornell), Peter Beak (University of Illinois), Victor Snieckus (University of Waterloo), Gideon Fraenkel (The Ohio State University), Scott Denmark (University of Illinois), Jay Siegel (UC—San Diego), Lloyd Jackman (Penn State), Dieter Seebach (ETH), and Donald Slocum (University of Western Kentucky) for helpful discussions and comments pertaining to this manuscript.

Supplementary Material Available: Table with details of the diffraction analysis, plots of atom labels, and tables of atomic coordinates, bond lengths and angles, and anisotropic thermal parameters for $[(LDA)_2TMEDA]_\infty$ (9 pages). Ordering information is given on any current masthead page.

(51) Dewar, M. J. S.; Thiel, W. *J. Am. Chem. Soc.* **1977**, *99*, 4899, 4907.
(52) Stewart, J. J. P. *QCPE 581.*
(53) Thiel, W.; Clark, T., unpublished results.
(54) Kaufmann, E.; Clark, T.; Schleyer, P. v. R. *J. Am. Chem. Soc.* **1984**, *106*, 1856. Sapse, A.-M.; Kaufmann, E.; Schleyer, P. v. R.; Gleiter, R. *Inorg. Chem.* **1984**, *23*, 1569.

Direct Formation of Highly Functionalized Allylic Organocopper Reagents from Allylic Chlorides and Acetates

Douglas E. Stack, Bryan T. Dawson, and Reuben D. Rieke*

Contribution from the Department of Chemistry, University of Nebraska-Lincoln, Lincoln, Nebraska 68588-0304. *Received October 21, 1991*

Abstract: The direct formation of highly functionalized allylic organocopper reagents has been carried out using a highly active form of zerovalent copper (Cu*). The cold-temperature reduction of CuCN·*n*LiX complexes by lithium naphthalenide in THF under an argon atmosphere produces the Cu* complex, which reacts rapidly with primary and secondary allyl chlorides at −100 °C with little homocoupling. Allyl, methallyl, and crotyl acetates also oxidatively add with Cu* at low temperatures to afford the corresponding organocopper reagent. Significantly, the allyl chlorides can contain a wide array of functional groups including ketones, α,β-unsaturated ketones, epoxides, alkyl acetates, esters, alkyl chlorides, nitriles, and carbamates. The cross-coupling of the highly functionalized allylic organocopper reagents with various electrophiles proceeds in excellent yields.

Introduction

Allylic organometallics have seen considerable use in organic synthesis for the formation of carbon–carbon bonds.[1] Although organocopper reagents have been used extensively in C–C bond formation,[2] their use in delivering an allylic ligand has been limited when compared to sp^3 and sp^2 ligands. The reasons for the confined use of allylic organocopper reagents lie in both the difficulty in their preparation and their limited thermal stability. Recently, significant progress has been made in both the understanding and the synthetic use of allylic organocopper reagents

Scheme I

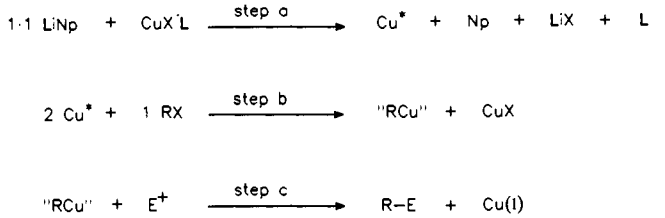

(1) (A) Courtois, G.; Miginiac, L. *J. Organomet. Chem.* **1974**, *69* 1. (b) Hoffmann, R. W. *Angew. Chem., Int. Ed. Engl.* **1982**, *21*, 555. (c) Biellmann, J. F.; Ducep, J. B. *Org. React. (N.Y.)* **1982**, *27*, 1. (d) Benkeser, R. A. *Synthesis* **1971**, *347*. (e) Chan, T. H.; Fleming, I. *Synthesis* **1979**, 763. (f) Schlosser, M. *Pure Appl. Chem.* **1988**, *60*, 1627. (g) Yamamoto, Y. *Acc. Chem. Res.* **1987**, *20*, 243.
(2) Reviews: (a) Posner, G. H. *Org. React. (N.Y.)* **1972**, *19*, 1. (B) Posner, G. H. *Org. React. (N.Y.)* **1975**, *22*, 253. (c) Posner, G. H. *An Introduction to Synthesis Using Organocopper Reagents*; Wiley: New York, **1980**. (d) Lipshutz, B. H. *Synthesis* **1987**, 325. (e) Lipshutz, B. H. *Tetrahedron* **1984**, *40*, 5005. (f) Normant, J. F. *Synthesis* **1972**, 63.

0002-7863/92/1514-5110$03.00/0